Vol 16 No 1, January 2007
1009-1963/2007/16(01)/0088-07

Chinese Physics

© 2007 Chin. Phys. Soc.
and IOP Publishing Ltd

Influence of spatiotemporal coupling on the capture-and-acceleration-scenario vacuum electron acceleration by ultrashort pulsed laser beam*

Lu Da-Quan(陆大全), Qian Lie-Jia(钱列加)†,
Li Yong-Zhong(李永忠), and Fan Dian-Yuan(范滇元)

Department of Optical Science and Engineering, Fudan University, Shanghai 200433, *China*

(Received 12 August 2005; revised manuscript received 12 June 2006)

This paper investigates the properties of the ultrashort pulsed beam aimed to the capture-and-acceleration-scenario (CAS) vacuum electron acceleration. The result shows that the spatiotemporal distribution of the phase velocity, the longitudinal component of the electric field and the acceleration quality factor are qualitatively similar to that of the continuous-wave Gaussian beam, and are slightly influenced by the spatiotemporal coupling of the ultrashort pulsed beam. When the pulse is compressed to an ultrashort one in which the pulse duration $T_{\mathrm{FWHM}} < 5T_0$, the variation of the maximum net energy gain due to the carrier-envelope phase is a crucial disadvantage in the CAS acceleration process.

Keywords: vacuum electron acceleration, ultrashort pulsed beam

PACC: 4170, 4260K, 4225B

1. Introduction

Due to the development of chirped-pulse amplification (CPA) technique, peta-watt (PW) short-pulse lasers with intensity of $10^{22}\mathrm{W/cm}^2$ are available in laboratories.[1−4] Because of the high intensity of the laser field, a number of methods have been proposed to accelerate the charged particles (especially electrons),[5−9] such as the wake-field electron acceleration, the plasma beat wave acceleration, inverse Cherenkov acceleration, etc. Among these methods, Ho *et al* demonstrates a mechanism of electron acceleration which is called capture-and-acceleration-scenario (CAS).[10−13] The basic physical mechanism of CAS acceleration is as follows: relativistic electrons are injected into a region where the phase velocity of the laser field is subluminal, thus the electrons can be trapped in the acceleration phase of the laser field for a sufficiently long time and receive considerable amount of energy from the laser field.

Although the high peak power provided by the ultrashort pulsed beam greatly benefits the CAS acceleration, the spatiotemporal coupling in the propagation makes the investigation of properties of the pulsed beam much more complicated than that of the continuous-wave (CW) beam. It has been proved that even in free space propagation the spatial and temporal dynamics cannot be analysed separately. Many phenomena caused by the spatiotemporal coupling have been reported in several papers,[14−22] which include the time-derivative effect, decrease of the optical period along the beam axis, pulse time delay, the red shift toward the beam periphery, and the spatially induced group-velocity dispersion, etc. We could reasonably expect that properties related to CAS acceleration, such as the phase velocity, the longitudinal component of the electric field, the acceleration quality factor, and the maximum net energy gain, should be influenced by the spatiotemporal coupling. Because of the importance of these properties in the CAS acceleration, the influence of spatiotemporal coupling should be investigated.

In this paper, based on the Gaussian pulsed Gaussian beam (GPGB), we investigate the properties of the pulsed beam which is related to the CAS acceleration. The spatiotemporal distribution of the phase velocity, the longitudinal component of the electric field and the acceleration quality factor (AQF) are

*Project supported by the Natural Science Foundation of China (Grant Nos 60538010, 10335030 and 10376009), the Science and Technology Commission of Shanghai, China (Grant Nos 05JC14005 and 05SG02), and the Graduate Science and Technology Innovation Foundation of Fudan University, China.

†Corresponding author. E-mail: ljqian@fudan.edu.cn

investigated. It shows that these properties is qualitatively similar to that of the CW Gaussian beam (GB), and are quantitatively influenced by the spatiotemporal coupling of the pulsed beam, especially when the full-width-at-half-maximum (FWHM) duration is shorter than 5 optical cycle. Furthermore, the maximum net energy gain of the injected electron from the pulsed beam is influenced by the carrier-envelope phase (CEP), and this influence is a crucial disadvantage in the CAS acceleration process which is driven by the ultrashort pulsed beam.

2. Preliminaries

In the CAS process, when electrons are injected into the electromagnetic (EM) field, their motion is determined by the relativistic Newton–Lorentz equation

$$\frac{\mathrm{d}\boldsymbol{P}}{\mathrm{d}t} = -e(\boldsymbol{E} + \boldsymbol{V} \times \boldsymbol{B}). \tag{1}$$

In this paper our aim is not the detailed numerical calculation of the movement of the injected electron, but the investigation of the properties of the pulsed laser beam related to the CAS acceleration. Therefore, our main discussion is based on the free propagation of the electromagnetic field. When the paraxial approximation is introduced, the propagation of the electric field $\boldsymbol{E} = \boldsymbol{E}_\perp + \boldsymbol{E}_z$ is governed by the paraxial wave equation

$$(\nabla_\perp^2 - \frac{1}{c^2}\partial_t^2)\boldsymbol{E} = 0, \tag{2}$$

where $\nabla_\perp^2 = \partial_x^2 + \partial_y^2$ is the transversal Laplacian. Equation (2) can be used to describe both the transverse field $\boldsymbol{E}_\perp$ and the longitudinal field $\boldsymbol{E}_z$. Frequently we firstly get $\boldsymbol{E}_\perp$, then by use of the equation

$$\nabla \cdot \boldsymbol{E} = 0, \tag{3}$$

we get the longitudinal electric field. According to Maxwell's equations, the magnetic field can be obtained by solving the equation

$$\nabla \times \boldsymbol{E} = -\partial_t \boldsymbol{B}. \tag{4}$$

As for the ultrashort pulsed beam, we introduce the local variables, $\tau = t - z/c$, $\varsigma = z$. We assume that the pulsed beam whose pulse duration is longer than one optical cycle, thus the ultrashort pulsed beam can be described by a carrier frequency ω_0 and an envelope $\boldsymbol{\Psi}$,[23–25] $\boldsymbol{E} = \boldsymbol{\Psi}(\boldsymbol{r}, \zeta, \tau)\exp(\mathrm{i}\omega_0\tau)$, $\boldsymbol{B} = \boldsymbol{\Phi}(\boldsymbol{r}, \zeta, \tau)\exp(\mathrm{i}\omega_0\tau)$, where $\omega_0 = 2\pi/T_0$ and T_0 is the optical oscillation period of the carrier frequency. The field envelope then satisfies the equations,

$$\left[\nabla_\perp^2 - 2\mathrm{i}k_0\partial_\zeta\left(1 - \frac{\mathrm{i}}{\omega_0}\partial_\tau\right)\right]\boldsymbol{\Psi}_\perp = 0, \tag{5}$$

$$\boldsymbol{\Psi}_\zeta = \frac{-\mathrm{i}}{k_0}\left(1 + \frac{\mathrm{i}}{\omega_0}\partial_\tau\right)\nabla_\perp \cdot \boldsymbol{\Psi}_\perp, \tag{6}$$

$$\boldsymbol{\Phi}(\boldsymbol{r}, \zeta, \tau) = \frac{\mathrm{i}}{\omega_0}\left(1 + \frac{\mathrm{i}}{\omega_0}\partial_\tau\right)\nabla \times \boldsymbol{\Psi}, \tag{7}$$

where $k_0 = \omega_0/c$. In the derivation of Eqs.(6) and (7), approximations $\left(1 - \frac{\mathrm{i}}{\omega_0}\partial_\tau\right)^{-1}\boldsymbol{\Psi}_\perp \cong \left(1 + \frac{\mathrm{i}}{\omega_0}\partial_\tau\right)\cdot\boldsymbol{\Psi}_\perp$ and $|\partial_\zeta\boldsymbol{\Psi}_\zeta| \ll |k_0\boldsymbol{\Psi}_\zeta|$ are introduced.

From Eqs.(6) and (7), the longitudinal electric field and the magnetic field, as well as their phases, can be easily obtained if the transversal electric field solution of Eq.(5) is known.

As can be seen in Eqs.(5)–(7), the term $\frac{\mathrm{i}}{\omega_0}\partial_\tau\boldsymbol{\Psi}_\perp$ stands for the spatiotemporal coupling of the pulsed beam. For a smooth pulse envelope, pulse duration Δt is a suitable measure of the typical variation time of the envelope. Thus the term $\left|\frac{\mathrm{i}}{\omega_0}\partial_\tau\boldsymbol{\Psi}_\perp\right| \sim \frac{1}{2\pi M}|\boldsymbol{\Psi}_\perp|$, where $M = \Delta t/T_0$, T_0 is the oscillation period of the carrier frequency. For the long or monochromatic pulsed beam, the term $\frac{\mathrm{i}}{\omega_0}\partial_\tau\boldsymbol{\Psi}_\perp$ is small and can be ignored, thus the pulsed beam can be written as a product of a pulse form and a beam expression. But for the pulsed beam with only few optical oscillation periods in the pulse duration, the spatiotemporal coupling cannot be ignored.

The advancing of the solid-state lasers and the CPA technique provides the high-peak-power ultrashort pulsed beam with only few or even one cycle oscillation in the pulse duration. When the pulse is short like this, the acceleration properties will be influenced by the spatiotemporal coupling in the pulsed beam. Then in the following sections, we will investigate the properties of the pulsed beam that are related to the CAS acceleration, such as the distribution of the phase velocity, the longitudinal component and the acceleration quality factor. And an important property of the ultrashort pulsed beam, i.e., the influence of the CEP on the net energy gain of electron, is discussed.

3. Phase velocity of ultra-short pulsed beam

For convenience of discussion, we assume the spectrum be a Gaussian one. Then in the temporal

domain, the linearly polarized GPGB can be written as[7]

$$\Psi_{\perp}^{(\mathrm{G})}(\boldsymbol{r},\zeta,\tau)=\exp\left[-\frac{t_{\mathrm{c}}^2}{\Delta t^2}\right]\frac{\mathrm{i}z_{\mathrm{R}}}{q(\zeta)}\exp\left[-\frac{\mathrm{i}k_0r^2}{2q(\zeta)}\right], \quad (8)$$

where $t_{\mathrm{c}}=\tau-\dfrac{r^2}{2cq}$ is the complex time. In Eq.(8), the time is a complex one t_{c} instead of the commonly description, in which the long pulse approximation is adopted and all the frequency components are multiplied by a common temporal factor such as $\exp\left[-\dfrac{\tau^2}{\Delta t^2}\right]$. As a result, in Eq.(8), the spatial and temporal characteristics affect each other during propagation, and this effect is the usually called spatiotemporal coupling. And we could reasonably expect that the spatiotemporal distribution of the phase velocity will be influenced by the spatiotemporal coupling.

The phase velocity of the pulsed beam is

$$V_{\mathrm{p}}=\frac{\partial_\tau\varphi(r,\varsigma,\tau)+\omega_0}{\sqrt{(\partial_x\varphi)^2+(\partial_y\varphi)^2+\left[\left(\dfrac{1}{c}\partial_\tau\varphi+k_0\right)-\partial_\varsigma\varphi\right]^2}}, \quad (9)$$

where φ is the phase of GPGB. Because of the complexity of the expression of the phase in Eq.(8), we write it as an alternative form

$$\varphi=\arctan\frac{\mathrm{Im}\left(\boldsymbol{\Psi}_{\perp}^{(\mathrm{G})}\right)}{\mathrm{Re}\left(\boldsymbol{\Psi}_{\perp}^{(\mathrm{G})}\right)}. \quad (10)$$

Based on Eqs.(8)–(10), we investigated the spatiotemporal distribution of the phase velocity in the GPGB.

The (r,ς) distribution of the phase velocity of GPGB is shown in Fig.1(a).

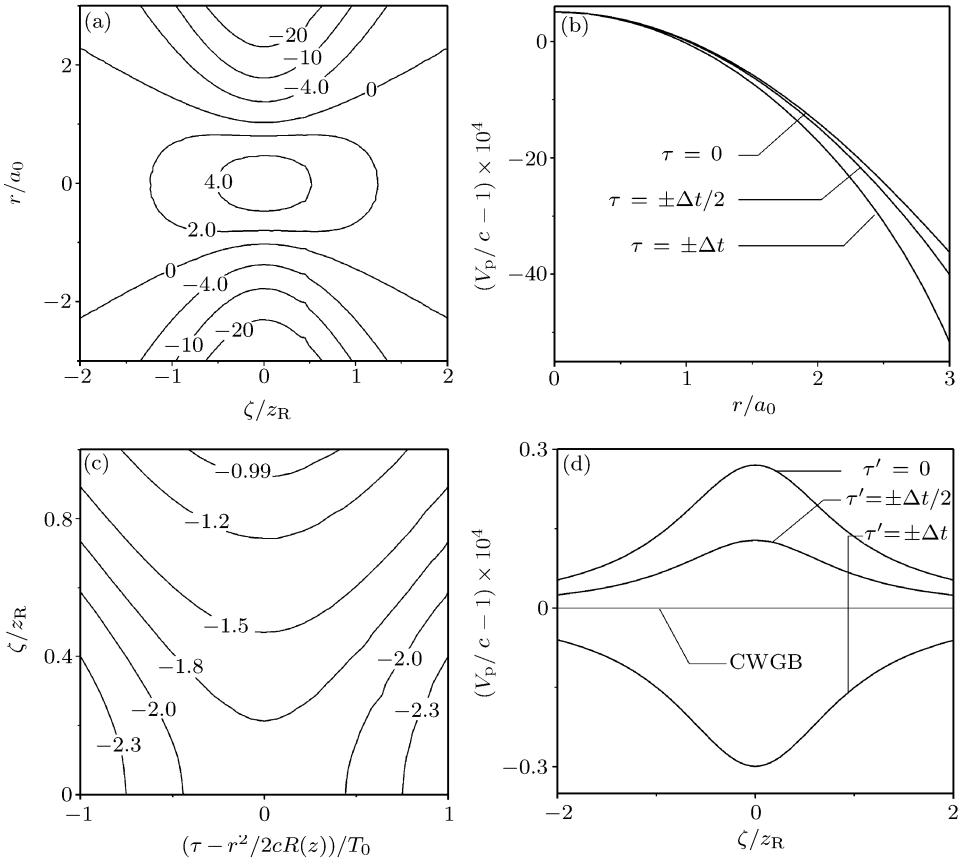


Fig.1. (a) The spatial distribution of $(V_{\mathrm{p}}/c-1)\times10^4$ at $\tau=0$. (b) The transverse distribution of $(V_{\mathrm{p}}/c-1)\times10^4$ at $\zeta=0$ for different time instants. (c) The distribution of $(V_{\mathrm{p}}/c-1)\times10^4$ at $r=1.2\,w(\zeta)$. To show the time delay of the distribution, the time coordinate is taken as $\tau'=\tau-r^2/2cR(\zeta)$ instead of τ. (d) The variation of $(V_{\mathrm{p}}/c-1)\times10^4$ alone the propagation distance ζ at $r=w(\zeta)$ for different time instants, and that of the CW GB is also drawn for comparison. In Figs.1(a)–1(d) the parameters is taken as $\Delta t=T_0, w_0=10\lambda_0$.

The distribution of the GPGB is qualitatively similar to that of the CW GB:[13] when $r = 0$, the phase velocity is superluminal, and the phase velocity decreases toward the beam periphery. Consequently, there is a subluminal region in the beam periphery. This property makes it possible for the CAS acceleration by use of the ultrashort pulsed beam. Because of the spatiotemporal coupling in the GPGB, there are quantitative differences between the spatiotemporal distribution of the phase velocity of the pulsed beam and that of the CW GB. And these differences are illustrated in Figs.1(b)–1(d).

In Fig.1(b), the transverse distribution of the phase velocity of the pulse centre ($\tau = 0$) is compared with that of the pulse leading ($\tau < 0$) and the pulse trail ($\tau > 0$) at the plane $\varsigma = 0$. It shows that the phase velocity is slightly different in various parts of the pulse. In the subluminal phase velocity region, the leading part and the tail part have smaller phase velocities. And the distribution of the phase velocity is symmetric about the pulse centre, i.e. $V_p(r, 0, \tau) = V_p(r, 0, -\tau)$.

Along with the propagation of the pulsed beam, the distribution of the phase velocity is no longer symmetric about $\tau = 0$. And just as the time delay of the pulse amplitude,[17] the symmetric centre is delayed by a factor $\tau_0 = \dfrac{r^2}{2cR(z)}$, where $R(z) = z[1 + (z/z_{\rm R})^2]^{1/2}$ is the radius of the wave front at the cross section z. This property is shown in Fig.1(c).

In Fig.1(d), we plot the distribution of the phase velocity alone $r = w(\varsigma)$, where $w(\varsigma) = w(0)\left[1 + \left(\dfrac{\varsigma}{z_R}\right)^2\right]^{1/2}$ is the beam width of the centre frequency at the cross section ς. Considering the time delay of the distribution of the phase velocity, we introduce a new temporal variable $\tau' = \tau - \tau_0$ in Fig.1(d). As for the CW GB, the phase velocity which is c at $r = w(\varsigma)$ and $r = w(\varsigma)$ can be regarded as the edge of the subluminal region. But in the pulsed beam, the phase is not equal to c at $r = w(\varsigma)$. As shown in Fig.1(d), at the time-delay shifted pulse centre, i.e., $\tau' = 0$, the phase velocity is superluminal at $r = w(\varsigma)$, which means that the region of the subluminal phase velocity is diminished. At the shifted pulse heading and the tail, the phase velocity at $r = w(\varsigma)$ decreases with the $|\tau'|$. When $|\tau'| = \Delta t/2$, the phase velocity is still superluminal. When $|\tau'|$ increases to Δt, the phase velocity is smaller than c and the subluminal phase velocity region is expanded into the $r < w(\varsigma)$ region.

In Fig.1 the pulse length is taken as $\Delta t = T_0$, then the FWHM duration $T_{\rm FWHM} \simeq 1.67T_0$. With the increase of pulse duration, the influence of spatiotemporal coupling on the distribution of the phase velocity becomes weaker. In our investigation, when $\Delta t > 3T_0 (T_{\rm FWHM} > 5T_0)$, the influence is very weak and can be neglected.

4. The spatiotemporal distribution of longitudinal component

When electrons are injected into the laser field, the acceleration properties is determined by the full EM field, including the transversal and longitudinal electric field as well as the magnetic field. But the previous research shows that the electron is accelerated mainly by the longitudinal electrical field.[13] This property makes the longitudinal electric field very important in the acceleration process.

From Eq.(7), the longitudinal component is determined by

$$\Psi_\zeta^{(\rm G)} = \frac{-{\rm i}}{k_0}\left(1 + \frac{\rm i}{\omega_0}\partial_\tau\right)\nabla_\perp \cdot \Psi_\perp^{(\rm G)}. \qquad (11)$$

In Fig.2(a), the transverse distribution of the longitudinal component at $\tau = 0, \zeta = 0$ cross section is drawn.

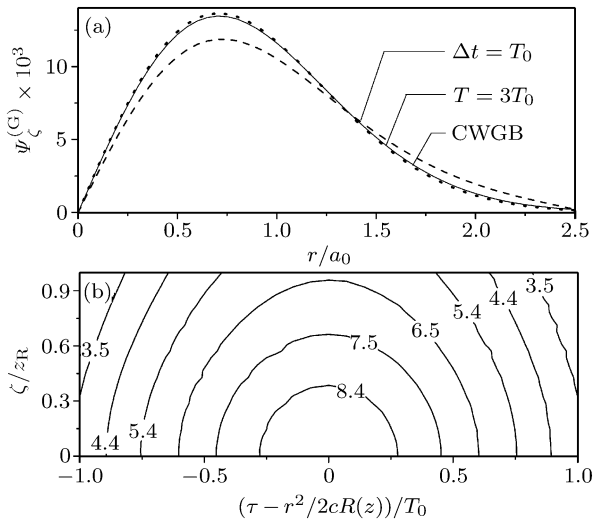


Fig.2. (a) The transverse distribution of the longitudinal component of the electric field $\Psi_\zeta^{(\rm G)} \times 10^3$ at $\zeta = 0, \tau = 0$ for different pulse duration Δt. (b) The distribution of $\Psi_\zeta^{(\rm G)} \times 10^3$ at $r = 1.2w(\zeta)$ with $\Delta t = T_0$. To show the time delay of the distribution, the time coordinate is taken as $\tau - r^2/2cR(\zeta)$ instead of τ. The parameter in Figs.2(a)–2(b) is taken as $w_0 = 10\lambda_0$.

And for comparison, we also drawn that of the CW GB. It shows that, at $\zeta = 0$, the transverse distribution of the longitudinal component of the pulsed beam is qualitatively similar to that of the CW GB: the longitudinal component is mainly distributed at the beam periphery of the transverse component. At $r \simeq 0.7w(\zeta)$, the longitudinal component arrives at its maximum. And this is true at $\zeta > 0$.

Quantitatively, as shown in Fig.2(a), the maximum of the longitudinal component of the GPGB is smaller than that of the CW GB. But at the periphery of the longitudinal component, the intensity of the longitudinal component of the GPGB is larger than that of the CW GB. This means that the spatiotemporal coupling shifts the energy of the longitudinal component of GPGB to the periphery. And the difference decreases with the increase of pulse duration, when $\Delta t > 3T_0 (T_{\rm FWHM} > 5T_0)$, the difference is so small that it can be neglected.

In Fig.2(b), it shows that there is also a time delay $\tau_0 = \dfrac{r^2}{2cR(z)}$ of the pulse centre of the longitudinal component, just as the time delay of the distribution of the phase velocity.

5. The acceleration quality factor

In the CAS acceleration, to make the injected electron accelerated effectively, there should be a region where: (i) the phase velocity is sufficiently low to trap electrons in the acceleration phase of the laser field for a sufficiently long time; (ii) the longitudinal component should have sufficiently high intensity to provide electrons with considerable account of energy. Therefore we introduce the acceleration quality factor (AQF) to present the acceleration capability of the laser field,[13]

$$Q = Q_0 m_v \Theta(m_v) \Psi_\zeta^{(\rm G)}, \tag{12}$$

where $m_v = 1 - \dfrac{V_{\rm p}}{c}$ presents the contribution from the phase velocity, $Q_0 = 10^7$. Considering that electrons cannot be trapped when $m_v > 0$, we introduce the Heaviside step function $\Theta(m_v)$.

The distribution of the AQF is shown in Fig.3(a). At the plane $\zeta = 0$, $\tau = 0$, where the intensity of the pulse is the maximum, the acceleration region is shifted a little to the beam periphery compared to that of the CW GB with the same intensity of the pulse peak. The maximum of the AQF of the pulsed beam is smaller than that of the CW GB. And at the periphery the AQF of the pulsed beam is larger than that of the CW GB. And this difference decreases with the pulse duration. When the pulse duration is increased to $\Delta t = 3t_0$ ($T_{\rm FWHM} = 5T_0$), the difference can be neglected.

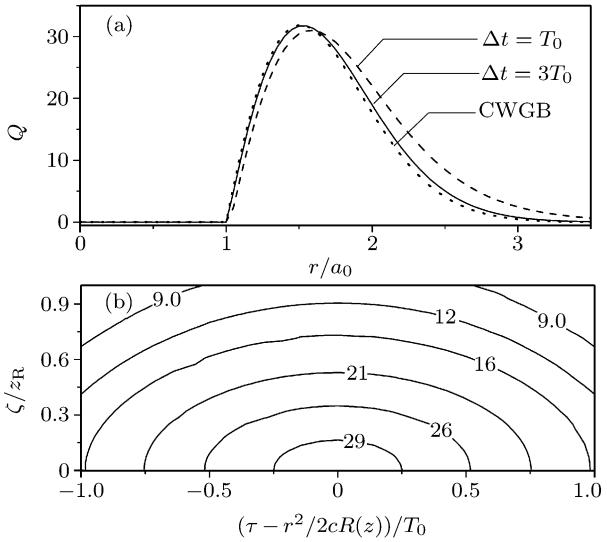


Fig.3. (a) The transverse distribution of the AQF at $\zeta = 0, \tau = 0$ for different pulse duration $\triangle t$. (b)The distribution of AQF at $r = 1.5w(\zeta)$ with $\Delta t = T_0$. To show the time delay of the distribution, the time coordinate is taken as $\tau - r^2/2cR(\zeta)$ instead of τ. The parameter in Figs.3(a) and 3(b) is taken as $w_0 = 10\lambda_0$.

As expected, the AQF of the pulse centre is the maximum, and that of the pulse trail and the pulse head is smaller than that of the centre. Thus, the AQF of the pulse can be looking as an AQF pulse. With the propagation of the pulse, there is also a time delay of the distribution of the AQF pulse, as shown in Fig.3(b).

6. Influence of the CEP on the net energy gain of the electron

The phase difference between the carrier wave and its pulse envelope, called the carrier–envelope phase (CEP) or the absolute phase, is an important parameter of the laser pulse. In this section we discuss the influence of CEP on the net energy gain of electrons. Assume that the electron trajectory angle is small compared to the diffraction angle. Therefore the energy gain is primarily due to the longitudinal

component of the electric field $\Psi_\zeta^{(\mathrm{G})}$, and the energy gain is approximately

$$W = -e\int \mathrm{d}\zeta \mathrm{Re}[\Psi_\zeta^{(\mathrm{G})}\exp(\mathrm{i}\omega_0\tau + \mathrm{i}\varphi_0)]. \qquad (13)$$

To get the accurate energy gain, Eq.(13) should be numerically integrated by using the exact orbits, and the difference between the velocity of electrons and the phase velocity of the pulsed beam should be considered. For convenience of discussion, the approximation adopted in Ref.[13] is introduced, and from Eq.(13), the approximate energy gain is $W[\mathrm{Mev}] \simeq 0.19a_0k_0w_0\exp\left[-\dfrac{\tau^2}{\Delta t^2}\right]\cos(\omega_0\tau+\varphi_0)$, where $a_0 = eE_0/(m\omega c)$ is the usually adopted parameter which is related to the intensity of the laser beam at the focus.

In Fig.4, we illuminate the influence of the CEP φ_0 on the maximum net energy gain for different pulse duration under the condition $w_0 = 10\lambda_0$. It shows that the maximum net energy gain is greatly influenced by the CEP when the FWHM pulse duration T_{FWHM} is about one or two cycles long. When $T_{\mathrm{FWHM}} = T_0$, the maximum net energy gain is reduced from 110MeV to 55MeV when the CEP is increased from 0 to π. This reduction is 50% of the maximum net energy gain when the CEP is 0. When $T_{\mathrm{FWHM}} = 2T_0$, the reduction is about 16%. The difference decreases rapidly with the pulse duration. When $T_{\mathrm{FWHM}} = 5T_0$, the difference is only 3%.

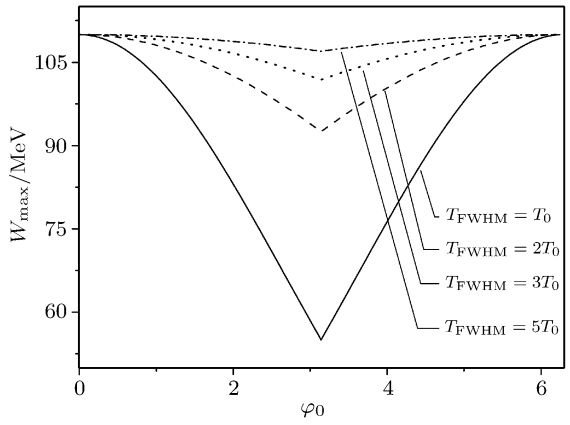


Fig.4. Variation of the maximum net energy gain $W_{\max}$ with the CEP φ_0 for different pulse duration.

Thus, although the compressed laser pulse can provide a considerably high peak power, when the pulse is compressed to an ultrashort one in which the FWHM pulse duration $T_{\mathrm{FWHM}} < 5T_0$, the variation of the maximum net energy gain with CEP is a disadvantage in the CAS acceleration process. In this case, to improve the availability of the pulsed beam and make the CAS acceleration the most efficient, the CEP should be precisely controlled.

7. Discussion and conclusion

In summary, we have investigated the properties of the ultrashort pulsed GB aimed to the CAS acceleration. It shows that the qualitative distribution of the phase velocity, the longitudinal component and the AQF are similar to that of the CW GB. This makes it possible to use the ultrashort pulsed beam to accelerate electrons. Quantitatively, the spatiotemporal coupling (i) makes the phase velocity of the pulse trail and head a little smaller than that of the pulse centre; (ii) shifts the subluminal phase region of the pulse centre, the energy of the longitudinal component of the electric field and the distribution of the AQF toward the beam periphery; (iii) decreases the maximum of the longitudinal component of the electric field and the AQF; (iv) induces the time delay $\tau_0 = \dfrac{r^2}{2cR(z)}$ of the distribution of phase velocity, the longitudinal electric field, and the AQF in the pulse. When the FWHM pulse duration $T_{\mathrm{FWHM}} > 5T_0$, the spatiotemporal coupling as well as the above influence is very weak and can be neglected. And the long pulse approximation can be adopted, i.e. the pulsed beam can be simply written as a product of a beam expression and a common temporal shape factor, in the investigation of the CAS acceleration process.

Furthermore, although the high peak power of the ultrashort pulsed beam greatly benefit the CAS acceleration, the influence of the CEP on the maximum net energy gain is a critical disadvantage when the FWHM pulse duration is shorter than 5 optical cycle. Therefore, if we want to introduce these ultrashort pulsed beam into the CAS acceleration process, besides the technique of large-band-width pulse amplification and pulse compression, the technique of CEP control is very important.

References

[1] Strickland D and Mourou G 1985 *Opt. Commun.* **56** 219

[2] Mourou G, Barty C P J and Perry M D 1998 *Phys. Today* **51** 22

[3] Perry M D, Pennington D, Stuart B C, Tietbohl G, Britten J A, Brown C, Herman S, Golick B, Kartz M, Miller J, Powell H T, Vergino M and Yanovsky V 1999 *Opt. Lett.* **24** 160

[4] Kienberger R, Hentschel M, Uiberacker M, Spielmann C, Kitzler M, Scrinzi A, Wieland M, Westerwalbesloh T, Kleineberg U, Heinzmann U, Drescher M and Krausz F 2002 *Science* **297** 1144

[5] Sprangle P, Esarey E and Krall J 1996 *Phys. Plasma* **3** 2183

[6] Sprangle P, Esarey E, Ting A and Joyce G 1988 *Appl. Phys. Lett.* **53** 2146

[7] Moore C I, Ting A, Mcnaught S J, Qiu J, Burris H R and Sprangle P 1999 *Phys. Rev. Lett.* **82** 1688

[8] Umstadter D, Chen S Y, Maksimchuk A, Mourou G and Wagner R 1996 *Science* **273** 472

[9] Gahn C, Tsakiris G D, Pukhov A, Meyer-ter-Vehn J, Pretzler G, Thirolf P, Habs D and Witte K J 1999 *Phys. Rev. Lett.* **83** 4772

[10] Wang J X, Ho Y K, Kong Q, Zhu L J, Feng L, Scheid S and Hora H 1998 *Phys. Rev.* E **58** 6575

[11] Wang P X, Ho Y K, Yuan X Q, Kong Q, Cao N, Sessler A M, Esarey E and Nishida Y 2001 *Appl. Phys. Lett.* **78** 2253

[12] Kong Q, Ho Y K, Cao N, Pang J, Wang P X and Shao L 2002 *Appl. Phys.* B **74** 517

[13] Pang J, Ho Y K, Yuan X Q, Cao N, Kong Q, Wang P X and Shao L 2002 *Phys. Rev.* E **66** 066501

[14] Belenov E M and Nazarkin A V 1994 *J. Opt. Soc. Am. A* **11** 168

[15] Ziolkowski R W and Judkins J B 1992 *J. Opt. Soc. Am.* A **9** 2021

[16] Wang Z, Zhang Z, Xu Z and Lin Q 1997 *IEEE J. Quantum Electron.* **33** 566

[17] Porras M A 1998 *Phys. Rev.* E **58** 1086

[18] Porras M A 1999 *J. Opt. Soc. Am.* B **16** 1468

[19] Hu W and Guo H 2002 *J. Opt. Soc. Am.* B **19** 49

[20] Peng R W and Fan D Y 2005 *Acta Phys. Sin.* **54** 2680 (in Chinese)

[21] Liu Z j and Lü B D 2003 *Chin. Phys.* **12** 55

[22] Lu D Q, Hu W, Yang Z J and Zheng Y Z 2004 *Acta Phys. Sin.* **53** 1063 (in Chinese)

[23] Brabec T and Krausz F 1997 *Phys. Rev. Lett.* **78** 3282

[24] Brabec T and Krausz F 2000 *Rev. Mod. Phys.* **72** 545

[25] Born M and Wolf E 1999 *Principles of Optics* (Cambridge: Cambridge University Press)